# Measurement of Lactose Repressor–Mediated Loop Formation and Breakdown in Single DNA Molecules

Laura Finzi* and Jeff Gelles†

In gene regulatory systems in which proteins bind to multiple sites on a DNA molecule, the characterization of chemical mechanisms and single-step reaction rates is difficult because many chemical species may exist simultaneously in a molecular ensemble. This problem was circumvented by detecting DNA looping by the lactose repressor protein of *Escherichia coli* in single DNA molecules. The looping was detected by monitoring the nanometer-scale Brownian motion of microscopic particles linked to the ends of individual DNA molecules. This allowed the determination of the rates of formation and breakdown of a protein-mediated DNA loop in vitro. The measurements reveal that mechanical strain stored in the loop does not substantially accelerate loop breakdown, and the measurements also show that subunit dissociation of tetrameric repressor is not the predominant loop breakdown pathway.

DNA looping, in which a protein or protein complex binds simultaneously to two separated sites on a DNA molecule, is a fundamental mechanism for the regulation of gene expression (*1*). For example, looping by the lactose repressor protein modulates transcription of the *Escherichia coli* lactose operon (*2*–*4*). To understand the molecular mechanisms of transcriptional regulation, it is necessary to examine the thermodynamics and kinetics of looping. Although the stabilities of loops formed by lactose repressor and other proteins have been characterized (*3*, *5*, *6*), the rates at which protein-mediated loops form and break down in vitro have not been measured. Such measurements are difficult with conventional biochemical techniques, which are restricted to observation of the population-averaged properties of large numbers of molecules. Here we describe direct, time-resolved detection of loop formation and breakdown in single DNA molecules. Single-molecule kinetic analysis (*7*) of these events helps discriminate between proposed mechanisms of loop breakdown.

To detect looping in individual DNA molecules, we used a tethered particle motion method, which consists of monitoring by light microscope digital image processing techniques the Brownian motion of a microscopic particle tethered by a single DNA molecule to a glass surface (*8*). We prepared a linear double-stranded DNA labeled at one end with digoxigenin and at the other end with biotin and containing two primary *lac* operators (DNA binding sites for the lactose repressor) separated by 305 base pairs (bp) (Fig. 1A). This operator arrangement produces stable repressor-mediated loops in vitro (*3*). We attached the digoxigenin-labeled DNA ends to a glass cover slip coated with an antibody to digoxigenin and subsequently labeled the opposite ends of the immobilized DNA molecules with avidin-conjugated polystyrene beads (0.226 μm in diameter) (*9*). Examination of the cover slips by differential interference contrast light microscopy revealed that most surface-attached beads displayed the restricted Brownian motion characteristic of beads linked to the cover slip by a flexible DNA tether (*8*). The surface density of DNA on the cover slip was sufficiently low to ensure that ≥~97% of the beads were attached to a single DNA molecule (*10*). Using previously developed image processing techniques (*11*), we measured the Brownian motion of the DNA-tethered beads (*12*). The motion of beads tethered by the two-operator DNA (Fig. 1A) is essentially constant in time (Fig. 2A), with measurements distributed in a single peak at ~73 nm (Fig. 2G).

When repressor is added to a preparation containing beads tethered by the two-operator DNA, repressor-mediated loops can form in the DNA molecules (Fig. 1C). We reasoned that looping would decrease the effective length of the DNA tether, thereby reducing the bead Brownian motion. Because the equilibrium of Fig. 1C is dynamic, individual molecules are expected to stochastically fluctuate between a short tether–low Brownian motion state (looped) and a long tether–high motion state (unlooped). Experimental data confirm this expectation. Fluctuations are observed in measurements of the Brownian motion of tethered beads in the presence of $1.0 \times 10^{-9}$ M repressor (Fig. 2, B to D). Frequency distributions of such measurements (for example, Fig. 2H) usually show in addition to the ~73-nm peak a new peak at ~48 nm, which is consistent with the presence of a discrete chemical state with a more restrictive DNA tether. We hypothesize that the ~73- and ~48-nm Brownian motion states correspond, respectively, to unlooped and looped forms of the DNA. This hypothesis is consistent with the following observations: (i) In control experiments in which repressor-mediated loop formation is prevented either by the addition of 1 mM isopropyl-β-D-thiogalactopyranoside (IPTG) (Fig. 2E) or by the use of a DNA containing a single operator (Figs. 1B and 2F), only one peak is observed in the data distributions (Fig. 2I). (ii) The magnitude of the Brownian motion of beads tethered by the one-operator DNA (~50 nm, Fig. 2, F and I) is similar to that in the ~48-nm putative looped state. This is expected because the length of the one-operator DNA is comparable with the effective length of the looped DNA (Fig. 1). (iii) Samples with the one-operator DNA in the absence of

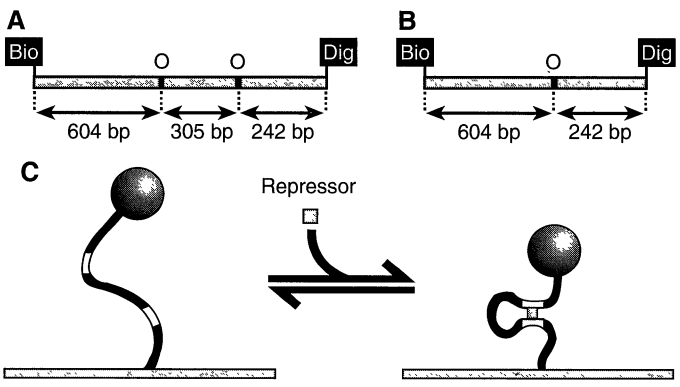


**Fig. 1.** (**A**) Labeled, two-operator double-stranded DNA used for single-molecule looping studies. (**B**) One-operator DNA used in control experiments. O, wild-type *lac* operator; Bio, biotin-labeled 5′ nucleotide; Dig, digoxigenin-labeled 3′ nucleotide (*20*). (**C**) Schematic of the light microscope specimens used to detect lactose repressor–mediated looping in single DNA molecules. Labeled DNA (black line) with two *lac* operators (white rectangles) tethers an avidin-conjugated 0.226-μm diameter polystyrene bead (circle) to a glass cover slip (shaded rectangle) coated with an antibody to digoxigenin. Looping of the DNA by a tetrameric repressor molecule (shaded square) decreases the effective length of the tether and consequently reduces bead Brownian motion.

Graduate Department of Biochemistry and the Center for Complex Systems, Brandeis University, Waltham, MA 02254, USA.

*Present address: Dipartimento di Biologia, Universita Statale di Milano, Via Celoria 26, Milano, 22100 MI, Italy.
†To whom correspondence should be addressed.

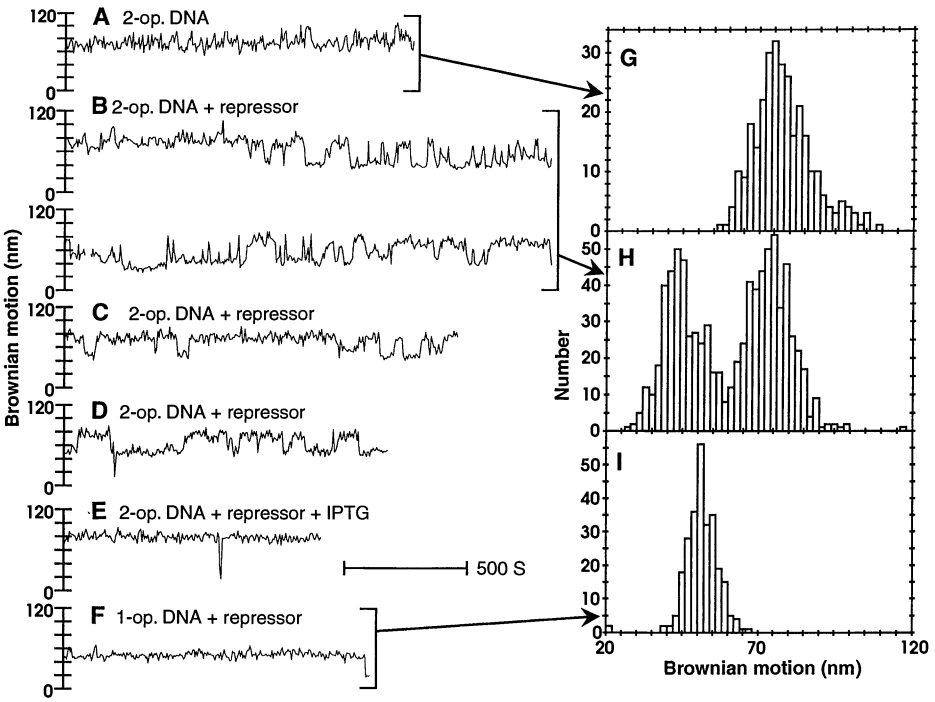


**Fig. 2.** Effect of repressor on the Brownian motion of DNA-tethered beads. (**A** to **F**) Each plot shows how the spatial range of motion of a single bead changes with time. (A) Bead tethered by two-operator (2-op.) DNA in the absence of repressor. (B to D) Three examples of beads tethered by two-operator DNA in the presence of $1.0 \times 10^{-9}$ M repressor. The second trace in (B) is a continuation of the first. (E) Bead tethered by two-operator DNA in the presence of $1.0 \times 10^{-9}$ M repressor and 1.0 mM IPTG (an inhibitor of repressor-operator specific binding). (F) Bead tethered by one-operator (1-op.) DNA in the presence of $1.0 \times 10^{-9}$ M repressor. (**G** to **I**) Frequency distributions of Brownian motion measurements from (A), (B), and (F), respectively. Spikes [for example, in (E)] in which the Brownian motion briefly decreases to near zero are caused by transient sticking of the bead to the cover slip surface.

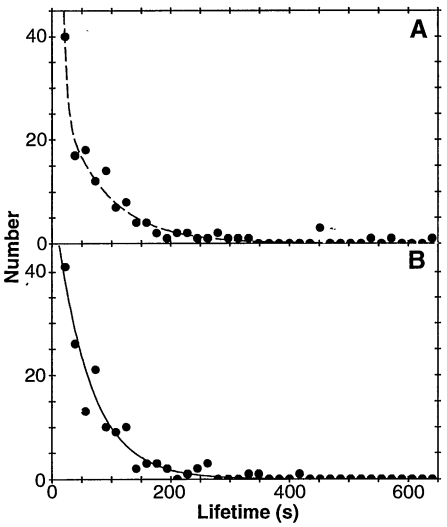


**Fig. 3.** Frequency distributions (noncumulative) of high Brownian motion (unlooped) and low Brownian motion (looped) state lifetimes for all data records with two-operator DNA in the presence of $1.0 \times 10^{-9}$ M repressor (see Table 1). The lengths of data records used in compilation of these distributions ranged between 4 and 75 min with a mean of 26 min. (**A**) Unlooped-state lifetimes (●), computer fit to a scaled biexponential probability distribution function (*15*) with lifetimes (weights) $\tau_1 = 77 \pm 6$ s [$a = 0.3 \pm 0.2$], $\tau_2 = 5.2 \pm 1.6$ s [$1 - a = 0.7$] (- - - -). (**B**) Looped-state lifetimes (●), computer fit to a scaled exponential probability distribution function (*15*) with lifetime $\tau = 58 \pm 2$ s (—).

repressor yielded data records and frequency distributions (*13*) indistinguishable from those obtained from samples with the one-operator DNA and a saturating concentration ($1.0 \times 10^{-9}$ M) (*3*) of repressor (Fig. 2, F and I). This demonstrates that binding of repressor to a single operator site does not cause (for example, by bending the DNA) a detectable change in bead Brownian motion. (iv) An algorithm that counts transitions between the ~73- and ~48-nm states (*14*) detects a high frequency of transitions in samples with repressor and two-operator DNA, and a zero or very low frequency in control samples (Table 1).

We characterized the kinetics of repressor-mediated DNA loop formation and breakdown by lifetime analysis of the single-molecule equilibrium data at $1.0 \times 10^{-9}$ M repressor (*15*). The frequency distribution of unlooped-state lifetimes (Fig. 3A) is fit better by the sum of two exponential terms than by a single exponential. This result is consistent with previous work that implies that the unlooped state consists of multiple chemical species in equilibrium (*5*, *16*). In contrast, the looped-state lifetimes (Fig. 3B) are well fit by a single exponential, consistent with the presence of only one looped species. The quality of the fit is evidenced by the close agreement of the decay constant [$\tau = 58 \pm 2$ (SE) s] with the mean of the measured looped-state lifetimes corrected (*17*) so as to include those lifetimes too short to be detected by our instrumentation ($\mu_{corr} = 69 \pm 6$ s). The latter is essentially unchanged ($\mu_{corr} = 73 \pm 11$ s) in experiments in which repressor concentration is reduced to $1.0 \times 10^{-10}$ M, suggesting that reactions involving the binding of free repressor molecules from solution do not significantly affect the rate at which the low (~48 nm) Brownian motion state decays. This argues against models in which the ~48-nm state is a composite of the looped and one or more distinct unlooped chemical species in rapid equilibrium, instead of the one looped species alone.

The apparent first-order unlooping rate constant ($k_{app} = 0.017$ s$^{-1}$, the reciprocal

**Table 1.** Transitions between high (~73-nm) and low (~48-nm) Brownian motion states of DNA-tethered beads.

| Additions | Data records* | Mean record length (min) | Total processed data (min) | Total transitions† | Mean transition frequency ± SD‡ (min$^{-1}$) |
|---|---|---|---|---|---|
| | | *Two-operator DNA* | | | |
| None | 10 | 16 | 165 | 0 | 0 |
| $1.0 \times 10^{-9}$ M repressor | 31 | 26 | 817 | 247 | 0.30 ± 0.02 |
| $1.0 \times 10^{-10}$ M repressor | 9 | 25 | 229 | 56 | 0.24 ± 0.03 |
| $1.0 \times 10^{-9}$ M repressor and 1 mM IPTG | 2 | 21 | 42 | 2 | 0.05 ± 0.03 |
| | | *One-operator DNA* | | | |
| $1.0 \times 10^{-9}$ M repressor | 12 | 22 | 269 | 8 | 0.03 ± 0.01 |

*Each data record is the time course of Brownian motion for an individual DNA-tethered bead, as in Fig. 2, A to F. †Number of crossings of a threshold set between the high and low Brownian motion states (*14*). The transition-counting procedure is expected to have a low but detectable false-positive rate due to noise in the data records. ‡Population standard deviations were calculated on the assumption that the transitions are Poisson distributed.

of $\tau$) places significant constraints on possible mechanisms of loop breakdown. Hsieh *et al.* (*3*) determined the rate constant of repressor dissociation from one-operator DNA to be ~0.006 $s^{-1}$ at ion and dimethylsulfoxide concentrations identical to those used here. This result accounts nearly completely for our observed unlooping rate because loop breakdown can occur by either of two equivalent protein-DNA dissociation reactions. This implies that the dissociation of repressor tetramers into dimers, a possible alternative pathway (*5*), cannot play a dominant kinetic role in loop breakdown under our experimental conditions. Similarly, the observations rule out a large acceleration of the repressor-DNA dissociation rate constant induced by the mechanical strain stored in the 305-bp DNA loop studied here (*18*).

We report direct measurements of the formation and breakdown kinetics of a repressor-mediated DNA loop. The single-molecule tethered particle motion method allows direct physical detection of loop formation, can be applied even when the system is at chemical equilibrium, and can distinguish the effects of biochemical heterogeneity from those of multiphasic kinetic processes. This method may prove useful in studying other protein-mediated DNA looping involved in transcriptional regulation and DNA recombination processes.

## REFERENCES AND NOTES


1. K. S. Matthews, *Microbiol. Rev.* **56**, 123 (1992); R. Schleif, *Annu. Rev. Biochem.* **61**, 199 (1992).
2. J. A. Borowiec, L. Zhang, S. Sasse-Dwight, J. D. Gralla, *J. Mol. Biol.* **196**, 101 (1987); E. Eismann, B. von Wilcken-Bergmann, B. Müller-Hill, *ibid.* **195**, 949 (1987); M. C. Mossing and M. T. Record Jr., *Science* **233**, 889 (1986); S. Oehler, E. R. Eismann, H. Krämer, B. Müller-Hill, *EMBO J.* **9**, 973 (1990).
3. W.-T. Hsieh, P. A. Whitson, K. S. Matthews, R. D. Wells, *J. Biol. Chem.* **262**, 14583 (1987).
4. H. Krämer *et al.*, *EMBO J.* **6**, 1481 (1987).
5. M. Brenowitz, A. Pickar, E. Jamison, *Biochemistry* **30**, 5986 (1991).
6. M. Brenowitz and E. Jamison, *ibid.* **32**, 8693 (1993); ———, A. Majumadar, S. Adhya, *ibid.* **29**, 3374 (1990).
7. D. Colquhoun and A. G. Hawkes, *Proc. R. Soc. London* **211**, 205 (1981).
8. D. A. Schafer, J. Gelles, M. P. Sheetz, R. Landick, *Nature* **352**, 444 (1991).
9. A coverslip flow chamber [E. Berliner *et al.*, *J. Biol. Chem.* **269**, 8610 (1994)] was incubated for 20 min with affinity-purified immunoglobulin G (IgG) to digoxigenin (20 μg/ml) (Boehringer) in buffered saline. After washing the flow chamber with 800 μl of buffer BB [10 mM tris-$Cl^-$ (pH 7.4), 200 mM KCl, 5% dimethylsulfoxide (DMSO), 0.1 mM EDTA, 0.2 mM dithiothreitol (DTT), and α-casein (0.1 mg/ml)], it was incubated for 1 hour with biotin- and digoxigen-labeled DNA in BB, and again washed with 800 μl of BB. Biotin-conjugated polystyrene beads (0.226 μm in diameter) were prepared, coated with avidin-DN (Vector Laboratories, Burlingame, CA), and purified as described [E. Berliner, E. C. Young, K. Andersen, H. K. Mahtani, J. Gelles, *Nature*, in press]. The chamber was washed with excess beads in BB lacking DMSO and DTT and incubated 20 min. Unattached beads were then flushed from the chamber with a solution of purified repressor in BB.
10. The DNA surface density was measured in an experiment that used DNA radiolabeled by inclusion of [α-$^{32}$P]deoxycytidine 5′-triphosphate (dCTP) in the polymerase chain reaction. When chambers were incubated with DNA at $<2 \times 10^{-9}$ M, the surface density was proportional to the applied DNA concentration. The DNA concentration ($1.0 \times 10^{-12}$ M) used for the microscope specimens was chosen to give a surface density of $1 \times 10^{-2}$ per square micrometer. At that density, ≤3% of DNA molecules have a nearest neighbor sufficiently close (within 1.04 μm) that the two molecules could attach to the same bead and ≤1% have a nearest neighbor sufficiently close (0.46 μm) that repressor could cross-link the two molecules in a sandwich complex (*4*), assuming that the DNA molecules are randomly distributed on the surface (*8, 19*). Additional experiments demonstrated that the DNA binding to the surface is specific [72 to 99% of binding was eliminated by pretreatment of the IgG-coated surface with digoxigenin-11-deoxyuridine 5′-triphosphate (dUTP)] and stable (only a small fraction of the DNA was released from the glass on incubation with 0.1 mM digoxigenin-11-dUTP for 1 hour).
11. Specimens with DNA-tethered beads were observed by video-enhanced differential interference contrast light microscopy at ~22°C and recorded on videotape, and the recordings were analyzed as described (*8*). In brief, we first averaged sequences of 128 consecutive video frames (4.3 s). The width of the bead image [the image size parameter (*8*)] in each averaged frame was determined by fitting the image with a parameterized image-shape function. Tethered bead Brownian motion (δ) was calculated with $\delta = S_T - \langle S_S \rangle$, where $S_T$ is the image size parameter of the tethered bead, $S_S$ is the image size parameter of an immobile bead from the same microscope field, and $\langle \ldots \rangle$ represents a time average over the full duration of the recording. Brownian motion data were smoothed with a three-point mean filter.
12. The Brownian motion measured by the tethered particle motion technique depends on the mean end-to-end distance of the segment of DNA that links the bead to the glass surface, as well as on the bead diameter and other geometrical factors. For the experimental conditions, bead size, and DNA length range used here, the measured Brownian motion is proportional to the DNA segment contour length, with a proportionality constant of 0.065 nm Brownian motion/(base pair tether length) (*19*). At the 4.3-s time resolution used here (*11*), the precision of the Brownian motion measurements is ~90 bp root mean square (*19*).
13. L. Finzi and J. Gelles, data not shown.
14. For each data record, we set a threshold to discriminate between the high and low Brownian motion states. For records with distributions displaying two peaks (for example, Fig. 2H), the threshold was set to the position of the local minimum between the peaks. On average, the minimum was 12 nm above the lower peak and 11 nm below the upper peak. For a record showing only a single lower or upper peak (for example, Fig. 2, I and G) the threshold was set at 12 nm above or 11 nm below the peak position, respectively. In each record, the algorithm counts the number of transitions across the threshold after revising the records [D. Colquhoun and B. Sakmann, *Nature* **294**, 464 (1981)] to eliminate events shorter than 12.9 s, twice the dead time of the smoothing filter (*17*).
15. Lifetimes of individual looped and unlooped states were measured by applying the thresholds described (*14*). Smoothing of the data precluded reliable detection of events of duration $< t_{min} = 12.9$ s; consequently, such events are not shown in Fig. 3 and were not fit. Remaining data were grouped in bins of width $w = 17.2$ s. A nonlinear least squares algorithm was used to fit the binned number ($n$)/lifetime ($t$) data to

$$n = \frac{Nw}{\tau} e^{(t_{min} - t)/\tau}$$

(scaled exponential probability distribution function) or

$$n = Nw \frac{a\tau_1^{-1} e^{-t/\tau_1} + (1 - a)\tau_2^{-1} e^{-t/\tau_2}}{a e^{-t_{min}/\tau_1} + (1 - a) e^{-t_{min}/\tau_2}}$$

(scaled biexponential probability distribution function), where $N$ is the total number of observed lifetimes and $a$ is a preexponential weighting factor (149 in Fig. 3A and 144 in Fig. 3B) (*17*).
16. In theory, each of the two operator sites could be vacant, occupied by a repressor dimer, or occupied by a repressor tetramer. Therefore, the unlooped state consists in principle of $3^2 = 9$ distinct chemical species in equilibrium and should exhibit a lifetime distribution equal to the sum of up to nine exponential terms. In practice, experimental noise and the large number of possible chemical species preclude accurate empirical determination of the number of terms (except that the number is ≥2), measurement of a complete set of time constants, or calculation (*7*) of single-step rate constants for the looping reactions or the reactions that interconvert unlooped species.
17. D. Colquhoun and F. J. Sigworth, in *Single-Channel Recording*, B. Sakmann and E: Neher, Eds. (Plenum, New York and London, 1983), pp. 191–263.
18. If the mechanical energy stored in the loop is substantial compared with the free energy of thermal excitation ($kT$), the mechanical strain in a repressor-mediated DNA loop can in principle accelerate either the dissociation of repressor from operator or the dissociation of repressor tetramers into dimers by altering the ground-state structure of the looped complex. It is not possible to exactly calculate the mechanical strain in a lactose repressor–induced loop because the distance between and orientations of the repressor DNA binding sites are not precisely known. However, we used the physical model of Brenowitz *et al.* (*5*) to roughly approximate the DNA bending free energy stored in the 305-bp loop used here as 4.1 kcal/mol (assuming a persistence length of 44 nm), approximately sevenfold larger than $kT$. Thus, although not observed with the lactose repressor–mediated loop studied here, mechanical strain could in principal accelerate unlooping reactions in other protein-mediated loops with similar geometries.
19. H. Yin, R. Landick, J. Gelles, *Biophys. J.* **67**, 2468 (1994).
20. DNAs were derived from the two-operator plasmid pRW490 (*3*) or the one-operator plasmid pLM2, which was prepared by ligating the 4363-bp and 305-bp Eco RI fragments of pRW490. We prepared biotin-labeled DNA by polymerase chain reaction from Sca I–digested plasmid template using primers 5′-biotin-dX-AGATCCAGTTCGATGT-3′ and 5′-ATAGTGGCTCCAAGTAGC-3′ (Midland) as previously described (*8*); unincorporated primers were removed by ultrafiltration [R. Higuchi, B. Krummel, R. K. Saiki, *Nucleic Acids Res.* **16**, 7351 (1988)]. The DNA 3′ ends were capped by the addition of 2′,3′-dideoxyadenosine 5′–triphosphate with terminal transferase. After removal of one end by Eco RV digestion and purification by gel electrophoresis, we used terminal transferase to label the uncapped end with digoxigenin-11-2′,3′-ddUTP (Boehringer). The labeled DNA was purified by phenol extraction and ethanol precipitation.
21. We thank L. B. McDaniel for cloning and preparing DNA and T. C. Boles and E. Berliner for advice and discussion. H. C. Pace (University of Pennsylvania) and K. S. Matthews (Rice University) generously provided repressor protein and plasmid DNAs. We also thank D. Thomas, T. Lyons, D. Peisach, and E. Young who performed preliminary studies for this project and C. Miller and K. S. Matthews for comments on the manuscript. Supported by grants from the Whitaker Foundation and NIH and by Scholar Awards to J.G. from the Lucille P. Markey Charitable Trust and the Searle Scholars Program.


28 June 1994; accepted 17 November 1994